Urban water storage capacity inferred from observed evapotranspiration recession

H.J. Jongen[1,2], G-J. Steeneveld[2], J. Beringer[3], A. Christen[4], N. Chrysoulakis[5], K. Fortuniak[6], J. Hong[7], J-W. Hong[8], C.M.J. Jacobs[9], L. Järvi[10,11], F. Meier[12], W. Pawlak[6], M. Roth[13], N.E. Theeuwes[14,15], E. Velasco[16], and A.J. Teuling[1]

[1]Hydrology and Quantitative Water Management, Wageningen University, Wageningen, The Netherlands.
[2]Meteorology and Air Quality, Wageningen University, Wageningen, The Netherlands.
[3]School of Agriculture and Environment, University of Western Australia, Crawley, Australia.
[4]Chair of Environmental Meteorology, Faculty of Environment and Natural Resources, University of Freiburg, Freiburg, Germany
[5]Foundation for Research and Technology Hellas, Institute of Applied and Computational Mathematics, The Remote Sensing Lab, Heraklion, Crete, Greece
[6]Department of Meteorology and Climatology, Faculty of Geographical Sciences, University of Łódź, Łódź, Poland.
[7]Department of Atmospheric Sciences, Yonsei University, Seoul, South Korea.
[8]Korea Environment Institute, Sejong, South Korea.
[9]Wageningen Environmental Research, Wageningen University and Research, Wageningen, The Netherlands.
*
[10]Institute for Atmospheric and Earth System Research / Physics, University of Helsinki, Helsinki, Finland.
[11]Helsinki Institute of Sustainability Science, University of Helsinki, Hesinki, Finland.
[12]Chair of Climatology, Technische Universität Berlin, Berlin, Germany.
[13]Department of Geography, National University of Singapore, Singapore.
[14]Department of Meteorology, University of Reading, Reading, United Kingdom.
[15]Royal Netherlands Meteorological Institute (KNMI), De Bilt, The Netherlands.
[16]Independent Research Scientist, Singapore.

Key Points:

- A new method is applied to infer urban water storage capacity from evapotranspiration recession.
- A first observational analysis of evaporation over cities worldwide reveals strong water limitation.
- Water storage capacity in cities is an order of magnitude smaller than in natural systems.

*Current affiliation: National Institute for Public Health and the Environment (RIVM), Bilthoven, The Netherlands

Corresponding author: Harro Jongen, harro.jongen@wur.nl

Abstract

Water storage plays an important role in mitigating heat and flooding in urban areas. Assessment of the capacity of cities to store water remains challenging due to the extreme heterogeneity of the urban surface. Traditionally, effective storage has been estimated from runoff. Here, we present a novel approach to estimate water storage capacity from recession rates of evaporation during precipitation-free periods. We test this approach for cities at neighborhood scale with eddy-covariance latent heat flux observations from fourteen contrasting sites with different local climate zones, vegetation cover and characteristics, and climates. We find effective water storage capacities to vary between 1.3–28.4 mm corresponding to *e*-folding timescales of 1.8–20.1 days. According to our results, urban water storage capacity is at least one order of magnitude smaller than the observed values for natural ecosystems, resulting in an evaporation regime characterised by extreme water limitation.

Plain Language Summary

Urban water storage plays an important role in mitigating urban flooding and affects urban heat via cooling through evapotranspiration. Determining the amount of water that can be stored in a city remains challenging due to the variability in urban landscapes. The methodology presented estimates this water storage based on how evapotranspiration declines over time during periods without precipitation. The estimated storage capacities amount to 1.3–28.4 mm, which is an order of magnitude smaller than in natural ecosystems.

1 Introduction

Cities face weather-related risks magnified by climate change, such as heatwaves and flooding (Wilby, 2007). At the same time, urbanization is expected to further increase the already large share of the world population living in cities (United Nations, 2018). In cities, air temperatures are typically higher than in the rural surroundings due to the Urban Heat Island effect (UHI) (Oke, 1982; Santamouris, 2014; Oke et al., 2017). The UHI can lead to increased energy demands, health issues and excess mortality (Stone Jr & Rodgers, 2001; Gabriel & Endlicher, 2011; Laaidi et al., 2011; Santamouris, 2015; Gasparrini et al., 2017). The UHI originates from the difference between the rural and urban energy balances due to lower albedo, radiation trapping, less vegetation, higher heat storage capacity and anthropogenic heat release (Oke, 1982). Because of its positive effect on evaporative cooling that is complemented by shading, urban vegetation is often given a central role in attempts to improve thermal comfort (Ennos, 2010). Indeed, higher vegetation fractions are associated with lower urban air and canopy temperatures (e.g. Gallo et al., 1993; Weng et al., 2004; Theeuwes et al., 2017), although in specific situations vegetation can cause higher temperatures (Meili et al., 2021a). It has been shown that actively expanding the vegetation fraction as part of urban renewal indeed has the potential to improve thermal comfort (Wei & Shu, 2020). Since vegetation-mediated cooling strongly depends on water availability for evapotranspiration (ET) (Avissar, 1992; Manoli et al., 2020), there is a need for methods to analyze and evaluate the effective storage in urban environments.

The generally low ET over urban areas also affects the water balance and make cities more prone to flooding. A high impervious surface fraction results in more storm water being discharged as runoff, which can also accumulate relatively fast (Arnold Jr & Gibbons, 1996; Fletcher et al., 2013). Consequently, more discharge decreases water availability for ET and thus indirectly contributes to the UHI (Taha, 1997; Zhao et al., 2014). The combination with heavy rainfall events leads to flood volumes that are 2–9 times higher than in rural areas (Paul & Meyer, 2001; Hamdi et al., 2011; Zhou et al., 2019). Due to the high population density and concentration of capital in cities, these floods cause considerable damage (Tingsanchali, 2012). This is likely to further increase due to increasing extreme precipitation (Huntington, 2006). Solutions have been proposed under various names such as Water Sensitive Urban Design (Wong, 2006), Low Impact Development (Qin et al., 2013), Sustainable Drainage Systems (Zhou, 2014), sponge cities (Gaines, 2016) and Nature Based Solutions (Somarakis et al., 2019). The common ground of these concepts is their focus on increasing infiltration and effective storage capacity, of which the latter at urban landscape scale is crucial for their performance (Graham et al., 2004; Qin et al., 2013). Therefore, an evaluation of the effective storage in cities is also needed in the light of flooding events.

Estimation of the urban water storage capacity is complicated by the strong heterogeneity of water sources for ET (Sailor, 2011). Previous studies have focused on ET from individual sources (e.g. Gash et al., 2008; Starke et al., 2010; Pataki et al., 2011; Ramamurthy & Bou-Zeid, 2014), as well as on their combined behaviour at street or neighborhood scale (e.g. Christen & Vogt, 2004; Jacobs et al., 2015; Meili et al., 2020, 2021b). In order to study ET on a neighborhood scale (order of hundreds of meters to 1–2 kilometers), flux measurements of latent heat with an associated footprint, such as those obtained by eddy covariance or scintillometry, are becoming increasingly popular. Due to the large size of the footprints, urban EC measurements often reflect different sources including impervious surfaces, vegetation, open water and all other sources of ET. Examples of cities for which such measurements have been studied are Arnhem (Jacobs et al., 2015), Basel (Christen & Vogt, 2004), Helsinki (Vesala et al., 2008), Melbourne (Coutts et al., 2007b), Seoul (Hong et al., 2019) and Singapore (Roth et al., 2017). Under water-limited conditions, ET observations contain information on storage. In one of the few studies directly linking urban ET and storage, Wouters et al. (2015) applied this principle to validate a new parametrization for the impervious contribution to urban water storage. However, the link between ET and footprint-scale urban water storage remains largely unexplored.

Recession analysis can be used to provide insight into the link flux observations and storage properties. From the 1970s, discharge recession analysis has been extensively used in groundwater and hillslope hydrology (e.g. Brutsaert & Nieber, 1977; Kirchner, 2009; Troch et al., 2013). Similarly, daily ET can be linked to water storage during a drydown, a period without precipitation creating water-limited conditions. Assuming that the ET decay is exponential, the e-folding time, or the timescale over which ET declines by 63%, reflects the available storage and resilience to droughts (Wetzel & Chang, 1987; Salvucci, 2001; Saleem & Salvucci, 2002). The reflected storage is defined by the methodology as the dynamic water storage capacity available to the atmosphere for ET, which includes soil moisture, intercepted precipitation and open water varying from lakes to puddles. In studies using daily ET over natural ecosystems, Teuling et al. (2006) and more recently Boese et al. (2019) found timescales ranging from 15 days for short vegetation to 35 days for forest ecosystems, and corresponding storage capacities in the range between 30 and 200 mm, with most sites in the range of 50 to 100 mm. A global-scale analysis of surface soil moisture recession by McColl et al. (2017) found timescales ranging from 2 to 20 days. Although valuable insight can be obtained from a comparison of urban and rural ET dynamics, recession analysis has not yet been applied to urban ET.

In this study, we extend the methodology developed by Teuling et al. (2006) to estimate footprint-scale water storage capacity based on EC observations of daily ET in cities. The methodology is applied to a new, unique collection of urban ET data from cities covering a range of climate conditions and with different urban land cover and structure. This allows for a first assessment of urban storage capacity across cities, an evaluation of how site characteristics (e.g. vegetation fraction) affect water storage, and a comparison of urban water storage to that of natural ecosystems.

2 Data and Methods

We analyze latent heat fluxes and auxiliary meteorological data obtained from eddy covariance flux towers at fourteen sites in twelve different cities to estimate water storage. Table 1 lists a number of important characteristics of each site, including key references. In these references, all observation sites and measurement details are fully described. The sites were chosen based on the length of the data record (minimum of a year), flux footprints representing typical urban neighborhoods without other land covers, and the availability of observed precipitation and latent heat fluxes. All sites are located in reasonably flat terrain. Most sites were located in mid-latitude climates, except Mexico City with a subtropical climate, Singapore with a tropical climate, and Helsinki, Łódź and Seoul with a continental climate. Vegetation fractions in the associated footprints vary between 6–56%.

Observations were reported in averaging periods of 10–30 min depending on the measurement protocol of each site. In this study, hourly averages were used to determine the timing of rainfall and 24-hour averages were used for the recession analysis. For all sites the quality control of the observed heat fluxes was performed by individual researchers responsible for their ET flux observation site. Although the exact methodology of the quality control differs per site, all fluxes have been properly tested in accordance with procedures published in literature (Aubinet et al., 2012).

During multi-day drydowns without water input via rainfall, drainage is typically very small, and the evolution in landscape-scale dynamic storage (S) can be simplified as:

$$\frac{dS(t)}{dt} = -\mathrm{ET}(t) \tag{1}$$

Under water-limitation, daily ET becomes a function of storage. For impervious surfaces in cities, the storage dynamics have been described by a $\frac{2}{3}$-power function contributing to ET, but depleting in a few hours of daytime (Masson, 2000; Ramamurthy & Bou-Zeid, 2014). ET from other sources will likely show a different behavior (Granger & Hedstrom, 2011; Nordbo et al., 2011), with ET from (urban) vegetation behaving more as a linear reservoir (Williams & Albertson, 2004; Dardanelli et al., 2004; Peters et al., 2011). Since impervious surfaces are typically quickly depleted, open water is constant and vegetation behaves more linear, we assume the flux footprint reflecting a mixture of different ET sources to effectively behave as a linear reservoir:

$$\mathrm{ET}(t) = f(S(t)) = cS(t) \tag{2}$$

in which $c = 1/\lambda$ is a proportionality constant. Combining Eq. 1 and Eq. 2 and solving the differential equation leads to an exponential response of ET:

$$\mathrm{ET}(t) = \mathrm{ET}_0 \exp\left(-\frac{t - t_0}{\lambda}\right) \tag{3}$$

where λ is the e-folding timescale, and ET_0 the initial ET. With these parameters the total dynamic storage volume S_0 in mm that would be depleted during a complete dry down ($t \to \infty$) is given by:

$$S_0 = \int_{t_0}^{\infty} \mathrm{ET}(t)\mathrm{d}t = \lambda \mathrm{ET}_0 \tag{4}$$

so that S_0 can be estimated using only ET observations. To further tailor this concept to urban environments, the anthropogenic moisture flux can be included. This flux

Table 1. Site characteristics and summary of regression analysis. The climate statistics are long-term means (1999–2019). The start and end of the indicated ranges for the parameters are respectively the 5^{th} and 95^{th} percentile of the median distribution from the bootstrapping re-samples. The value in brackets is the median itself. (LCZ Stewart and Oke (2012): 1 = compact high-rise, 2 = compact mid-rise, 3 = compact low-rise, 5 = open mid-rise, 6 = open low-rise, F_v: surface fraction covered by vegetation in a 500 m radius around the measurement site, z_s: height of sensors above ground level, z_H: mean building height, ET_0: initial evapotranspiration, *lambda*: *e*-folding timescale, $t\frac{1}{2}$: half-life, S_0: effective, dynamic water storage capacity)

City	Lat. (deg)	Lon. (deg)	Köppen-Geiger climate	Avg. temp. (deg C)	Ann. prec. (mm)	LCZ	F_v (%)	z_s (m)	z_H (m)	Start	End	Source	Nr. of dry-downs	Total days	ET_0 (mm d^{-1})	λ (day)	$t\frac{1}{2}$ (day)	S_0 (mm)
Amsterdam	52.37	4.89	Cfb	9.2	805	2	15	40	14	05-2018	10-2020	Ronda et al. (2017) Steeneveld et al. (2019)	15	61	0.9 – 1.8 (1.4)	3.4 – 16.4 (4.5)	2.4 – 11.3 (3.1)	5.0 – 17.0 (7.3)
Arnhem	51.98	5.92	Cfb	9.4	778	2	12	23	11	05-2012	12-2016	Jacobs et al. (2015)	46	183	0.7 – 1.0 (0.8)	2.5 – 4.2 (3.0)	1.8 – 2.9 (2.1)	2.3 – 3.8 (3.0)
Basel (AESC)	47.55	7.6	Cfb	10	778	2	27	39	17	06-2009	12-2020	Lietzke et al. (2015)	120	500	0.8 – 1.0 (0.9)	4.2 – 5.6 (5.1)	2.9 – 4.0 (3.5)	3.6 – 4.9 (4.4)
Basel (KLIN)	47.56	7.58	Cfb	10	778	2	27	41	17	05-2004	12-2020	Schmutz et al. (2016)	158	661	1.0 – 1.2 (1.1)	4.9 – 6.8 (5.9)	3.4 – 4.7 (4.1)	5.4 – 7.8 (6.5)
Berlin (ROTH)	13.32	52.46	Cfb	9.1	570	6	56	40	17	06-2018	09-2020	Vulova et al. (2021)	7	33	0.4 – 0.9 (0.6)	4.8 – 11.0 (7.9)	3.3 – 7.6 (5.5)	1.3 – 9.9 (6.3)
Berlin (TUCC)	13.33	52.51	Cfb	9.1	570	5	31	56	20	07-2014	09-2020	Jin et al. (2020) Vulova et al. (2021)	36	149	0.3 – 0.8 (0.5)	3.0 – 5.2 (3.7)	2.1 – 3.6 (2.6)	1.4 – 3.6 (3.0)
Helsinki	60.33	24.96	Dfb	5.1	650	6	54	31	20	01-2006	12-2018	Vesala et al. (2008) Karsisto et al. (2016)	45	202	1.2 – 1.8 (1.6)	3.7 – 6.1 (4.4)	2.5 – 4.2 (3.1)	6.0 – 11.0 (8.5)
Heraklion (HECKOR)	35.34	25.13	Csa	17.8	464	3	12	27	11.3	Nov-16	May-21	Stagakis et al. (2019)	5	24	0.4 – 2.0 (0.5)	1.8 – 13.3 (6.5)	1.3 – 9.2 (4.5)	1.5 – 13.2 (2.8)
Łódź	51.76	19.45	Dfb	7.9	564	5	31	37	11	07-2006	09-2015	Fortuniak et al. (2013)	57	261	0.9 – 1.6 (1.3)	4.0 – 5.4 (4.4)	2.8 – 3.7 (3.1)	3.8 – 6.9 (5.8)
Melbourne (Preston)	-37.73	145.01	Cfb	14.8	666	5	38	40	6	08-2003	11-2004	Coutts et al. (2007b) Coutts et al. (2007a)	2	9	1.6 – 2.1 (1.9)	2.6 – 13.2 (7.9)	1.8 – 9.2 (5.5)	5.5 – 21.3 (13.4)
Mexico City	19.4	-99.18	Cwb	15.9	625	2	6	37	9.7	06-2011	09-2012	Velasco et al. (2011) Velasco et al. (2014)	8	49	0.7 – 1.5 (1.3)	5.5 – 16.5 (10.4)	3.8 – 11.5 (7.2)	5.8 – 21.9 (9.5)
Seoul	37.54	127.04	Dwa	11.9	1373	1	40	30	20	03-2015	02-2016	Hong et al. (2019) Hong et al. (2020)	10	59	0.6 – 2.0 (1.3)	2.3 – 9.9 (6.5)	1.6 – 6.9 (4.5)	3.3 – 10.7 (6.1)
Singapore	1.31	103.91	Af	26.8	2378	3	15	24	10	03-2013	03-2014	Velasco et al. (2013) Roth et al. (2017) Harshan et al. (2017)	7	40	1.3 – 1.6 (1.4)	4.6 – 20.1 (8.2)	3.2 – 14.0 (5.7)	7.7 – 28.4 (11.3)
Vancoucer	49.23	-123.08	Csb	9.9	1283	6	35	28	5	05-2008	07-2017	Christen et al. (2011)	67	308	1.2 – 1.4 (1.3)	6.5 – 8.9 (7.3)	4.5 – 6.2 (5.1)	7.1 – 9.5 (8.3)

can contribute substantially to ET, in particular during long, dry periods (Grimmond & Oke, 1986; Moriwaki et al., 2008; Miao & Chen, 2014), and includes processes like transport, heating, cooling (indoor), human metabolism and irrigation, which do not directly depend on rainfall. Variation in the daily averages of these processes, except for irrigation, can be expected to be negligible over the course of one drydown. Thus, to account for these processes we added a constant base term to Equation 3. Since this model yields parameters in compliance with the requirements explained below for only one drydown, we conclude that including this part of the anthropogenic moisture flux does not improve the physical representation of the city. As mentioned earlier, irrigation cannot be expected to be constant, while in some cities (e.g. Vancouver (Grimmond & Oke, 1986; Järvi et al., 2011) and Melbourne (Barker et al., 2011)) its contribution to ET can be considerable during long dry periods. We adapt the methodology in two ways to prevent irrigation affecting the results. First we limit the maximum duration of a drydown to 10 days decreasing the chance of irrigation. This also reduces the influence of the tail of the drydown on ET_0. Second we require an R^2 above 0.3, which is not achieved if irrigation causes ET to suddenly rise.

To estimate the parameters λ and ET_0, we identified all periods without precipitation for at least three continuous days, since three data points are the minimum requirement for an exponential fit (Figure 1). In order to preserve the information in ET during the first hours after rainfall (in case of low λ), we start the 24-hour averaging bins directly after the rainfall event, regardless of its magnitude. The bin-average is assigned to the middle of the day (e.g. the first bin is assigned to 0.5 day since rainfall). We exclude hours with an average shortwave incoming radiation below 10 $\mathrm{W\,m^{-2}}$ (i.e. nighttime), since during the night ET tends to be low. No gap-filling was applied, and only bins with at least 70% of data for daytime hours were analyzed. For the longest time series (Basel (KLIN)), requiring 70% instead of 100% increased the sample size by 48% respectively, while the median of the water storage capacities only changed by 25%. Further lowering the threshold did not increase data availability. Given the minimal effect on the results and potential to increase the sample size, 70% provides more information especially regarding cities with a shorter measurement period without compromising the results.

The ET observations were log-transformed so that a linear model based on Equation 3 could be fitted trough every individual drydown using the method of least squares, resulting in values for λ and ET_0 for each drydown. With increasing R^2, the parameters converge until $R^2 \approx 0.3$ (not shown), which shows drydowns with a lower R^2 are less reliable. In addition, the parameters are required to be physically plausible meaning positive λ and ET_0, but below 35 days (maximum found by Teuling et al. (2006)) respectively 10 $\mathrm{mm\,d^{-1}}$. Also, the average temperature during a drydown needs to exceed 0°C to exclude snow conditions, which is strict enough, confirmed by a check against snow records. To quantify the uncertainty of the estimated parameters complying with all criteria, we applied bootstrapping using 5000 re-samples containing 90% of the estimates. The confidence interval is defined as the 5^{th} and 95^{th} percentile of the median distribution from the re-samples.

With λ and ET_0 the storage capacity is calculated according to Equation 4 (shaded area in Figure 1). The calculated storage corresponds to the total storage capacity, when the storage capacity is assumed to be completely filled after every rainfall event. Drydowns occurring during all seasons are included and analyzed for a seasonal effect, since the water storage available to the atmosphere may change due to for example leaf phenology. Since it is not feasible to measure the water storage capacity in a complete urban footprint, this methodology offers the most direct estimation of the urban water storage. To investigate the possible impact of day-to-day variation or change in energy availability on the results, we repeated the recession analysis based on evaporative fraction

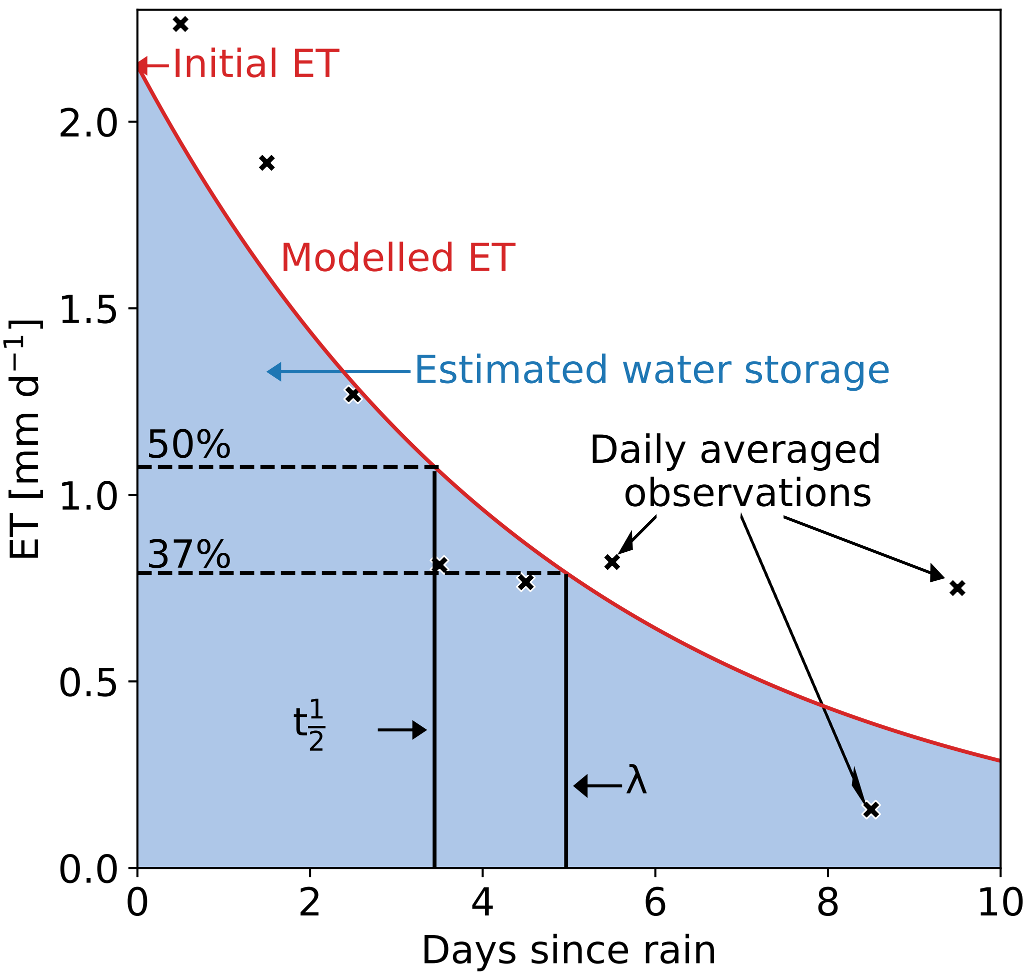

Figure 1. Illustration of the recession analysis. 24-hour aggregated ET versus the number of days following the last hour of precipitation for an example drydown from the Seoul data set with the fitted recession curve. Note that the fit was obtained by a linear fit on log-transformed data (see Data and Methods). In the figure the parameters are indicated.

(Gentine et al., 2007) multiplied by the average available energy over the drydown, which we included in the supplementary information (Table S1 and Figure S1 and S2).

3 Results

In Figure 2, the individual drydowns (in grey) show a good resemblance of the characteristic behaviour of the recession confirming the exponential behaviour. In general, ET is quickly decaying within days after rainfall in all LCZ's represented in our sample, indicating urban ET is generally strongly limited by water availability even on the first day after rainfall. As all cities respond similarly, this confirms the qualitative, decaying relation during a drydown. The spread of the observations is higher than the uncertainty, which is the result of a seasonal dependency. The uncertainty is visibly higher in cities with shorter measurement periods, since shorter periods inevitably mean smaller samples of drydowns. For Arnhem, Basel (AESC and KLIN), Berlin (Roth and TUCC), Helsinki, Łódź and Vancouver, observations are available for more than two full years resulting in narrow uncertainty bands. In contrast to the uncertainty bands for the sites with records of less than two years (Amsterdam, Melbourne, Mexico City, Seoul and Singapore), which are as wide as the range of observations. In some panels (e.g. Amsterdam and Helsinki), we observe two groups of curves with distinct slopes, for which we found no explanation in seasonality, energy availability, temperature and pre-drydown rainfall (amount and timing).

In Table 1, an overview of the parameters is given for the 583 drydowns that complied with all criteria. Of the total number of 1606 drydowns, 540 are excluded because of a negative λ and 151 because of a λ above 35 days. All drydowns had a positive ET_0, and only three exceeded 10 $\mathrm{mm\,d^{-1}}$. Snow conditions potentially influenced 132 drydowns, which are thus excluded. Finally, 700 drydowns did not meet the minimum R^2 of 0.3. The remaining drydowns yielded initial evapotranspiration between 0.3–2.1 $\mathrm{mm\,d^{-1}}$ and e-folding timescales between 1.8–20.1 days with the majority below 10.4 days, corresponding to half-lives of 1.3–14.0 and 7.2 days. The related storage capacities appear to be between 1.3–28.4 mm with the majority below 13.4 mm. As mentioned before, the length of the measurement period determines the magnitude of the uncertainty, which for S_0 varies from 1.2 mm in Basel (AESC) to 20.7 mm in Singapore (Figure 2).

For all sites, we find a considerable spread in the ET observations (Figure 2), which recurs in the estimated S_0 values. In Figure 3, S_0 is plotted against the month of the drydown, showing a very distinct seasonal dependency explaining why the spread in observations exceeds the uncertainty. Both ET_0 and λ, on which S_0 is based, show similar behaviour (not shown). Melbourne is shifted to fit the seasonality, as it is situated on the southern hemisphere. Since Singapore is close to the equator, it is not expected to show seasonal effect, which is confirmed lack of pattern in the points in Figure 3. Any connection between S_0 and the site characteristics in Table 1 and climatic variables among which precipitation regime is overshadowed by the seasonal dependency covering the full range of S_0 (Table 1), as we illustrate in the supplementary material (Figure S3 and S4). It is unfortunately not possible to eliminate the influence of this dependency by focusing on one season due to the steep slope, and not by focusing on one month due to the low data density. Only after omitting half of the cities based on the number of drydowns, a relation between S_0 and site characteristics is visible (Supplementary material Figure S5).

4 Discussion

In contrast with the results from this study found in urban areas, Teuling et al. (2006) found timescales ranging from 15–35 days and storage varying between 30 and 150 mm for forests and grassland with a similar methodology. When the urban parameter values found in this study are compared with these timescales and storage capacities (1.8–20.1 days and 1.3–28.4 mm), it is clear that both the timescales and storage capacities are higher in rural areas. McColl et al. (2017) have analyzed soil moisture drydowns in a global study using satellite data with a resolution too coarse to explicitly resolve individual cities, thus resembling rural values. Although their timescales with values from 2–20 days are closer to ours, it must be noted the temporal resolution is one in every three days and their observations only regard the first few centimeters instead of the root zone. Also, the satellite product in their research is known to underestimate the timescales compared to in-situ observations (Rondinelli et al., 2015; Shellito et al., 2016). Hence, the results show that both λ and S_0 are an order of magnitude smaller in cities indicating shorter timescales and lower storage capacities in urban areas regardless of their climate and vegetation fraction.

The applied methodology relies on a set of assumptions and limitations that confine its utilization. Since the method is observation-based, the reliability of the measurements is an important factor in this confinement. Eddy covariance is a sophisticated method

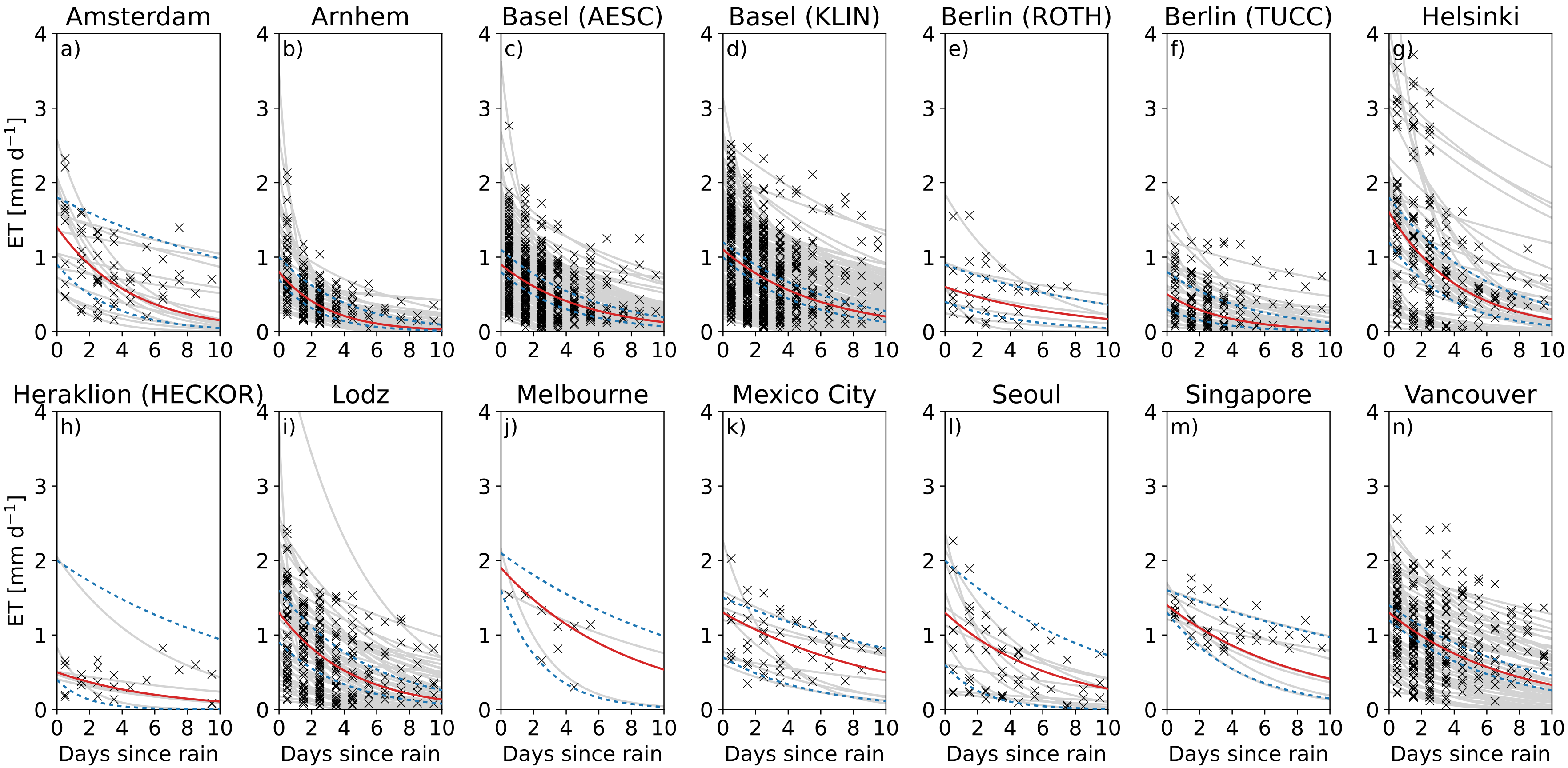

Figure 2. Daily average *ET* versus the day after the last precipitation with in red (continuous) the recession curve using the median parameter values, in blue (dotted) the 5$^{\text{th}}$ and 95$^{\text{th}}$ percentile of the median distribution from the bootstrapping re-samples, and in light grey all individual drydowns. The parameters of the fitted curves are shown in Table 1

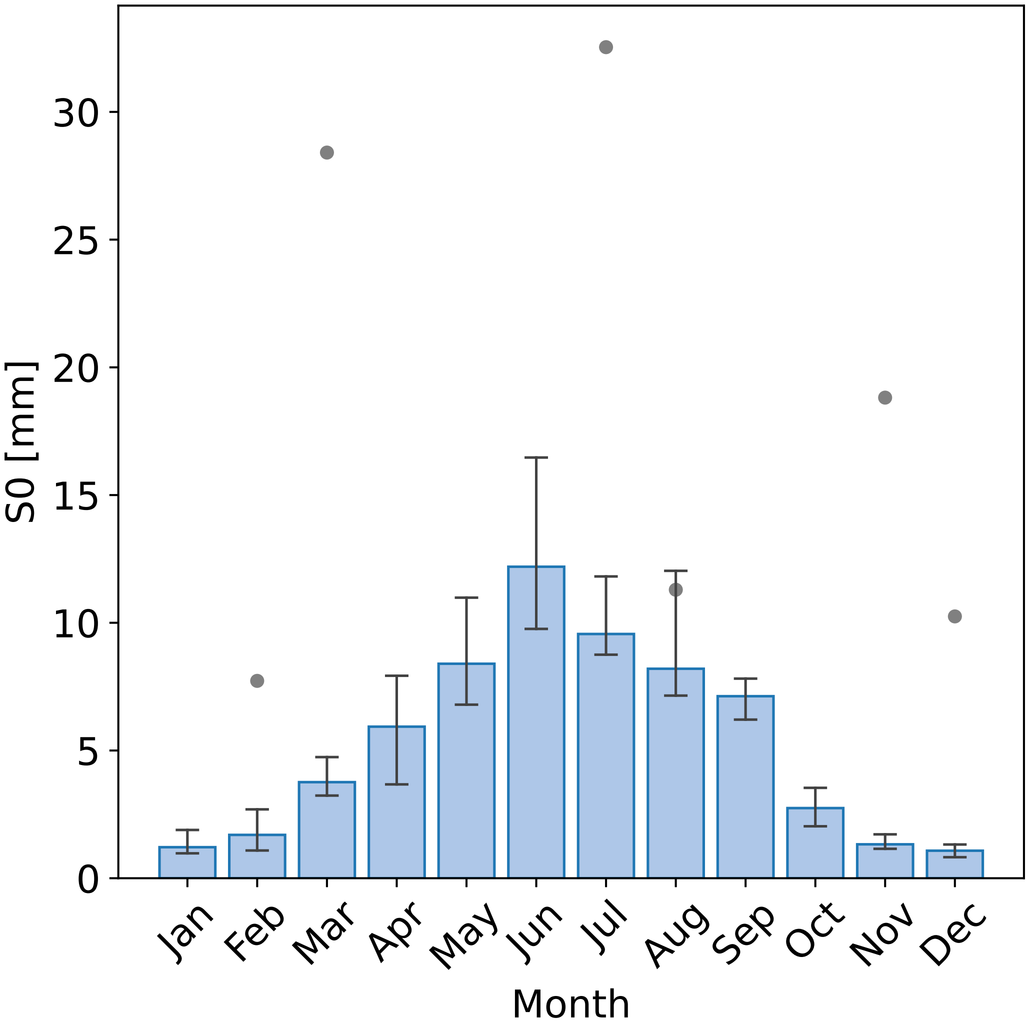

Figure 3. The seasonal dependency of S_0 for the sites on the northern hemisphere (Melbourne is included shifted by half a year) in blue and for Singapore as grey dots. The uncertainty is determined similarly as in Figure 2.

for measuring fluxes, but comes with a set of potential challenges in cities (Velasco & Roth, 2010; Feigenwinter et al., 2012; Järvi et al., 2018). By carefully selecting locations and applying quality control, these problems are minimized. All sites have an observation height well above the mean building height (see Table 1), and measure in the inertial sublayer. This reduces the variability in flux measurements in response to the heterogeneity of the monitored footprint, which is induced by the many, unevenly distributed surfaces with different characteristics and water storage capacities in the urban landscape. The only site in this research that includes a non-homogeneous footprint is Seoul, for which the observations are filtered by wind direction to exclude a nearby forest. Additionally, the long bins and quality control keep the influence of sudden fluctuations to a minimum.

Interception ET was an important consideration in the design of the methodology, since the high ET during the first day of a drydown can be largely attributed to this phenomenon (Savenije, 2004). Interception ET is a concept originally developed for forest environments, where interception is defined as water intercepted by the canopy. However, the concept can also be applied in urban environments with the more general definition of a temporary storage space only filled directly after rainfall (e.g. Grimmond & Oke, 1991; Gerrits, 2010; Oke et al., 2017). The volume of this temporary space is affected by urban design choices, such as the porosity of building materials and the slope of roofs. By calibrating an impervious-storage parameterization, (Wouters et al., 2015) estimated this storage to be between 1 and 1.5 mm for a site in Toulouse with little vegetation cover (8%). In order to capture the peak at the beginning of the recession caused by interception ET, the starting time of the 24-hour bins is not fixed but made dependent on rainfall, which can be during either day or night. Due to a low energy availability at night, relative to daytime more water may be drained and thus less interception might be evaporated. Since all parameters are independent of the starting hour of the bins (not shown), a bias due to the starting hour can be ruled out.

The methodology assumes that at the start of a drydown the storage capacity is completely full. A partly empty storage capacity would lead to an underestimation of the capacity, as less water is available for ET. We have compared the magnitude of the rain event before a drydown with the resulting parameters and found no correlation. Since the storage can be refilled by a series of events separated by dry days, we plotted the found parameters against the Antecedent Precipitation Index (API) (Fedora & Beschta, 1989). The API takes into account rainfall occurring during preceding days (here limited to 20), but also shows no correlations with the parameters. Therefore, the assumption of a completely filled storage is tangible and no selection has been performed based on rainfall event size.

The small storage capacity in cities shows their water balance is altered. Despite the limitations of the methodology discussed above, the estimates show the clear contrast between water storage capacity in urban and rural areas. The presented water storage estimation method has potential to offer an intriguing comparative analyses between less distinctive urban sites. The data presented here are not sufficient to substantiate, but do indicate their existence. In order to coin the larger potential and establish empirical relations between site characteristics and storage capacity, future research will need to focus on including longer records from more cities and applying soil moisture observations as a reference. Urban flux records are scarce both in number and length, as was previously indicated by Grimmond and Christen (2012), but their availability is improving. Additionally, very wet climates, such as Singapore's, only sporadically satisfy the conditions of the methodology increasing the necessity of long observational records. Soil moisture observations are available for only three sites in this study (Berlin, Singapore and Vancouver), but could indicate storage conditions. Earth observation data could help to improve data availability and scale the research up to the city level. To establish robust relations, future research will need to include many more cities with records of at least two years.

5 Conclusion

The timescales of ET recession observed in urban environments are considerably shorter than in rural environments. This is related to the storage capacity, which is also found to be lower. Timescales of cities are within 1.8–20.1 days with the majority below 10.4 days and storage capacities range between 1.3–28.4 mm with the majority below 13.4 mm. Both are an order of magnitude smaller than the values found in rural areas. We were unable to analyze differences between cities to vegetation fraction, local climate zone or climate for two reasons. Firstly, the seasonal dependency in the storage capacities is as strong as the total found variation. Secondly, the number of sites is limited, and for about half of them no more than one year of data is available. When provided with more data, the presented water storage capacity method has the potential to establish robust empirical relations explaining the differences between cities.

Acknowledgments

Harro Jongen acknowledges this research was supported by the WIMEK PhD grant 2020. The observations have been supported by Amsterdam Institute for Advanced Metropolitan Solutions (AMS Institute, project VIR16002), Netherlands Organisation for Scientific Research (NWO) Project 864.14.007 (Amsterdam), "Climate Proof Cities" within the second phase of the Knowledge for Climate Program, co-financed by the Dutch Ministry of Infrastructure and the Environment, the strategic research program KBIV 'Sustainable spatial development of ecosystems, landscapes, seas and regions', funded by the Dutch Ministry of Economic Affairs, Agriculture and Innovation, Wageningen University and Research Centre (Project KB-14-002-005) (Arnhem), Deutsche Forschungsgemeinschaft (DFG) grant SCHE 750/8 and SCHE 750/9 within Research Unit 1736 "Urban Climate and Heat Stress in Mid Latitude Cities in View of Climate Change (UCaHS)" and the research programme "Urban Climate Under Change ([UC]^2)", funded by the German Ministry of Research and Education (FKZ 01LP1602A) (Berlin), ICOS-Finland and CarboCity (grant no. 321527) funded by the Acedamy of Finland (Helsinki), Municipality of Heraklion (Contract 105, 26/5/2020), K. Politakos processing additional data (Heraklion), National Institute of Ecology and Climate Change (INECC) and Mexico City's Secretariat for the Environment through the Molina Center for Energy and the Environment (MCE2) (Mexico City), National Research Foundation of Korea Grant from the Korean Government (MSIT) (NRF-2018R1A5A1024958) (Seoul), National Research Foundation and the National University of Singapore (research grant R-109-000-091-112) (Singapore), Discovery Grants of the Natural Science and Engineering Research Council of Canada (NSERC), the Canada Foundation for Innovation (CFI) and the Canadian Foundation for Climate and Atmospheric Sciences (CFCAS) (Vancouver).

The data that support the findings of this study are openly available in data.4tu at http://doi.org/10.4121/13686973. (will be available upon acceptance and are now part of the Supporting Information)

References

Arnold Jr, C. L., & Gibbons, C. J. (1996). Impervious surface coverage: the emergence of a key environmental indicator. *Journal of the American planning Association*, *62*(2), 243–258.

Aubinet, M., Vesala, T., & Papale, D. (2012). *Eddy covariance: a practical guide to measurement and data analysis.* Springer Science & Business Media.

Avissar, R. (1992). Conceptual aspects of a statistical-dynamical approach to represent landscape subgrid-scale heterogeneities in atmospheric models. *Journal of Geophysical Research: Atmospheres*, *97*(D3), 2729–2742.

Barker, F., Faggian, R., & Hamilton, A. J. (2011). A history of wastewater irrigation in Melbourne, Australia. *Journal of Water Sustainability*, *1*(2), 31–50.

Boese, S., Jung, M., Carvalhais, N., Teuling, A. J., & Reichstein, M. (2019). Carbon–water flux coupling under progressive drought. *Biogeosciences*, *16*(13), 2557–2572.
Brutsaert, W., & Nieber, J. L. (1977). Regionalized drought flow hydrographs from a mature glaciated plateau. *Water Resources Research*, *13*(3), 637–643.
Christen, A., Coops, N., Crawford, B., Kellett, R., Liss, K., Olchovski, I., ... Voogt, J. (2011). Validation of modeled carbon-dioxide emissions from an urban neighborhood with direct eddy-covariance measurements. *Atmospheric Environment*, *45*(33), 6057–6069.
Christen, A., & Vogt, R. (2004). Energy and radiation balance of a central European city. *International Journal of Climatology: A Journal of the Royal Meteorological Society*, *24*(11), 1395–1421.
Coutts, A. M., Beringer, J., & Tapper, N. J. (2007a). Characteristics influencing the variability of urban co2 fluxes in Melbourne, Australia. *Atmospheric Environment*, *41*(1), 51–62.
Coutts, A. M., Beringer, J., & Tapper, N. J. (2007b). Impact of increasing urban density on local climate: Spatial and temporal variations in the surface energy balance in Melbourne, Australia. *Journal of Applied Meteorology and Climatology*, *46*(4), 477–493.
Dardanelli, J. L., Ritchie, J., Calmon, M., Andriani, J. M., & Collino, D. J. (2004). An empirical model for root water uptake. *Field Crops Research*, *87*(1), 59–71.
Ennos, R. (2010). Urban cool. *Physics World*, *23*(08), 22.
Fedora, M., & Beschta, R. (1989). Storm runoff simulation using an antecedent precipitation index (API) model. *Journal of hydrology*, *112*(1-2), 121–133.
Feigenwinter, C., Vogt, R., & Christen, A. (2012). Eddy covariance measurements over urban areas. In M. Aubinet, T. Vesala, & D. Papale (Eds.), *Eddy covariance a practical guide to measurement and data analysis* (p. 377-397). Dordrecht: Springer Netherlands.
Fletcher, T. D., Andrieu, H., & Hamel, P. (2013). Understanding, management and modelling of urban hydrology and its consequences for receiving waters: A state of the art. *Advances in water resources*, *51*, 261–279.
Fortuniak, K., Pawlak, W., & Siedlecki, M. (2013). Integral turbulence statistics over a central European city centre. *Boundary-layer meteorology*, *146*(2), 257–276.
Gabriel, K. M., & Endlicher, W. R. (2011). Urban and rural mortality rates during heat waves in Berlin and Brandenburg, Germany. *Environmental pollution*, *159*(8-9), 2044–2050.
Gaines, J. M. (2016). Water potential. *Nature*, *531*(7594 S1), S54–S54.
Gallo, K., McNab, A., Karl, T. R., Brown, J. F., Hood, J., & Tarpley, J. (1993). The use of a vegetation index for assessment of the urban heat island effect. *Remote Sensing*, *14*(11), 2223–2230.
Gash, J., Rosier, P., & Ragab, R. (2008). A note on estimating urban roof runoff with a forest evaporation model. *Hydrological Processes: An International Journal*, *22*(8), 1230–1233.
Gasparrini, A., Guo, Y., Sera, F., Vicedo-Cabrera, A. M., Huber, V., Tong, S., ... others (2017). Projections of temperature-related excess mortality under climate change scenarios. *The Lancet Planetary Health*, *1*(9), e360–e367.
Gentine, P., Entekhabi, D., Chehbouni, A., Boulet, G., & Duchemin, B. (2007). Analysis of evaporative fraction diurnal behaviour. *Agricultural and forest meteorology*, *143*(1-2), 13–29.
Gerrits, A. M. J. (2010). *The role of interception in the hydrological cycle.* PhD thesis. (TU Delft, http://resolver.tudelft.nl/uuid:7dd2523b-2169-4e7e-992c-365d2294d02e)
Graham, P., Maclean, L., Medina, D., Patwardhan, A., & Vasarhelyi, G. (2004). The

role of water balance modelling in the transition to low impact development. *Water Quality Research Journal*, *39*(4), 331–342.

Granger, R., & Hedstrom, N. (2011). Modelling hourly rates of evaporation from small lakes. *Hydrology and Earth System Sciences*, *15*(1), 267–277.

Grimmond, & Christen, A. (2012). Flux measurements in urban ecosystems. *FluxLetter*.

Grimmond, & Oke, T. R. (1986). Urban water balance: 2. results from a suburb of Vancouver, British Columbia. *Water Resources Research*, *22*(10), 1404–1412.

Grimmond, & Oke, T. R. (1991). An evapotranspiration-interception model for urban areas. *Water Resources Research*, *27*(7), 1739–1755.

Hamdi, R., Termonia, P., & Baguis, P. (2011). Effects of urbanization and climate change on surface runoff of the Brussels Capital Region: a case study using an urban soil–vegetation–atmosphere-transfer model. *International Journal of Climatology*, *31*(13), 1959–1974.

Harshan, S., Roth, M., Velasco, E., & Demuzere, M. (2017). Evaluation of an urban land surface scheme over a tropical suburban neighborhood. *Theoretical and applied climatology*, *133*(3-4), 867–886.

Hong, J.-W., Hong, J., Chun, J., Lee, Y. H., Chang, L.-S., Lee, J.-B., … Joo, S. (2019). Comparative assessment of net co 2 exchange across an urbanization gradient in Korea based on eddy covariance measurements. *Carbon balance and management*, *14*(1), 13.

Hong, J.-W., Lee, S.-D., Lee, K., & Hong, J. (2020). Seasonal variations in the surface energy and co2 flux over a high-rise, high-population, residential urban area in the East Asian monsoon region. *International Journal of Climatology*.

Huntington, T. G. (2006). Evidence for intensification of the global water cycle: review and synthesis. *Journal of Hydrology*, *319*(1-4), 83–95.

Jacobs, C., Elbers, J., Brolsma, R., Hartogensis, O., Moors, E., Márquez, M. T. R.-C., & van Hove, B. (2015). Assessment of evaporative water loss from Dutch cities. *Building and environment*, *83*, 27–38.

Järvi, L., Grimmond, C., & Christen, A. (2011). The surface urban energy and water balance scheme (suews): Evaluation in los angeles and vancouver. *Journal of Hydrology*, *411*(3-4), 219–237.

Järvi, L., Rannik, U., Kokkonen, T. V., Kurppa, M., Karppinen, A., Kouznetsov, R. D., … Wood, C. R. (2018). Uncertainty of eddy covariance flux measurements over an urban area based on two towers. *Atmospheric Measurement Techniques*, *11*(10), 5421–5438. Retrieved from `https://amt.copernicus.org/articles/11/5421/2018/` doi: 10.5194/amt-11-5421-2018

Jin, L., Schubert, S., Fenner, D., Meier, F., & Schneider, C. (2020). Integration of a building energy model in an urban climate model and its application. *Boundary-Layer Meteorology*, 1–33.

Karsisto, P., Fortelius, C., Demuzere, M., Grimmond, C. S. B., Oleson, K., Kouznetsov, R., … Järvi, L. (2016). Seasonal surface urban energy balance and wintertime stability simulated using three land-surface models in the high-latitude city Helsinki. *Quarterly Journal of the Royal Meteorological Society*, *142*(694), 401–417.

Kirchner, J. W. (2009). Catchments as simple dynamical systems: Catchment characterization, rainfall-runoff modeling, and doing hydrology backward. *Water Resources Research*, *45*(2).

Laaidi, K., Zeghnoun, A., Dousset, B., Bretin, P., Vandentorren, S., Giraudet, E., & Beaudeau, P. (2011). The impact of heat islands on mortality in Paris during the August 2003 heat wave. *Environmental health perspectives*, *120*(2), 254–259.

Lietzke, B., Vogt, R., Feigenwinter, C., & Parlow, E. (2015). On the controlling factors for the variability of carbon dioxide flux in a heterogeneous urban environment. *International journal of climatology*, *35*(13), 3921–3941.

Manoli, G., Fatichi, S., Bou-Zeid, E., & Katul, G. G. (2020). Seasonal hysteresis of surface urban heat islands. *Proceedings of the National Academy of Sciences*, *117*(13), 7082–7089.

Masson, V. (2000). A physically-based scheme for the urban energy budget in atmospheric models. *Boundary-layer meteorology*, *94*(3), 357–397.

McColl, K. A., Wang, W., Peng, B., Akbar, R., Short Gianotti, D. J., Lu, H., ... Entekhabi, D. (2017). Global characterization of surface soil moisture drydowns. *Geophysical Research Letters*, *44*(8), 3682–3690.

Meili, N., Manoli, G., Burlando, P., Bou-Zeid, E., Chow, W. T., Coutts, A. M., ... others (2020). An urban ecohydrological model to quantify the effect of vegetation on urban climate and hydrology (UT&C v1. 0). *Geoscientific Model Development*, *13*(1), 335–362.

Meili, N., Manoli, G., Burlando, P., Carmeliet, J., Chow, W. T., Coutts, A. M., ... Fatichi, S. (2021a). Tree effects on urban microclimate: Diurnal, seasonal, and climatic temperature differences explained by separating radiation, evapotranspiration, and roughness effects. *Urban Forestry & Urban Greening*, *58*, 126970.

Meili, N., Manoli, G., Burlando, P., Carmeliet, J., Chow, W. T., Coutts, A. M., ... Fatichi, S. (2021b). Tree effects on urban microclimate: Diurnal, seasonal, and climatic temperature differences explained by separating radiation, evapotranspiration, and roughness effects. *Urban Forestry & Urban Greening*, *58*, 126970. Retrieved from `https://www.sciencedirect.com/science/article/pii/S1618866720307871` doi: https://doi.org/10.1016/j.ufug.2020.126970

Miao, S., & Chen, F. (2014). Enhanced modeling of latent heat flux from urban surfaces in the noah/single-layer urban canopy coupled model. *Science China Earth Sciences*, *57*(10), 2408–2416.

Moriwaki, R., Kanda, M., Senoo, H., Hagishima, A., & Kinouchi, T. (2008). Anthropogenic water vapor emissions in Tokyo. *Water Resources Research*, *44*(11).

Nordbo, A., Launiainen, S., Mammarella, I., Leppäranta, M., Huotari, J., Ojala, A., & Vesala, T. (2011). Long-term energy flux measurements and energy balance over a small boreal lake using eddy covariance technique. *Journal of Geophysical Research: Atmospheres*, *116*(D2).

Oke, T. R. (1982). The energetic basis of the urban heat island. *Quarterly Journal of the Royal Meteorological Society*, *108*(455), 1–24.

Oke, T. R., Mills, G., Christen, A., & Voogt, J. A. (2017). *Urban climates.* Cambridge University Press.

Pataki, D. E., McCarthy, H. R., Litvak, E., & Pincetl, S. (2011). Transpiration of urban forests in the Los Angeles metropolitan area. *Ecological Applications*, *21*(3), 661–677.

Paul, M. J., & Meyer, J. L. (2001). Streams in the urban landscape. *Annual review of Ecology and Systematics*, *32*(1), 333–365.

Peters, E. B., Hiller, R. V., & McFadden, J. P. (2011). Seasonal contributions of vegetation types to suburban evapotranspiration. *Journal of Geophysical Research: Biogeosciences*, *116*(G1).

Qin, H.-p., Li, Z.-x., & Fu, G. (2013). The effects of low impact development on urban flooding under different rainfall characteristics. *Journal of environmental management*, *129*, 577–585.

Ramamurthy, P., & Bou-Zeid, E. (2014). Contribution of impervious surfaces to urban evaporation. *Water Resources Research*, *50*(4), 2889–2902.

Ronda, R., Steeneveld, G., Heusinkveld, B., Attema, J., & Holtslag, A. (2017). Urban finescale forecasting reveals weather conditions with unprecedented detail. *Bulletin of the American Meteorological Society*, *98*(12), 2675–2688.

Rondinelli, W. J., Hornbuckle, B. K., Patton, J. C., Cosh, M. H., Walker, V. A., Carr, B. D., & Logsdon, S. D. (2015). Different rates of soil drying after rainfall are observed by the SMOS satellite and the south fork in situ soil moisture

network. *Journal of Hydrometeorology*, *16*(2), 889–903.
Roth, M., Jansson, C., & Velasco, E. (2017). Multi-year energy balance and carbon dioxide fluxes over a residential neighbourhood in a tropical city. *International Journal of Climatology*, *37*(5), 2679–2698.
Sailor, D. J. (2011). A review of methods for estimating anthropogenic heat and moisture emissions in the urban environment. *International journal of climatology*, *31*(2), 189–199.
Saleem, J. A., & Salvucci, G. D. (2002). Comparison of soil wetness indices for inducing functional similarity of hydrologic response across sites in Illinois. *Journal of Hydrometeorology*, *3*(1), 80–91.
Salvucci, G. D. (2001). Estimating the moisture dependence of root zone water loss using conditionally averaged precipitation. *Water Resources Research*, *37*(5), 1357–1365.
Santamouris, M. (2014). Cooling the cities–a review of reflective and green roof mitigation technologies to fight heat island and improve comfort in urban environments. *Solar energy*, *103*, 682–703.
Santamouris, M. (2015). Analyzing the heat island magnitude and characteristics in one hundred Asian and Australian cities and regions. *Science of the Total Environment*, *512*, 582–598.
Savenije, H. H. (2004). The importance of interception and why we should delete the term evapotranspiration from our vocabulary. *Hydrological Processes*, *18*(8), 1507–1511.
Schmutz, M., Vogt, R., Feigenwinter, C., & Parlow, E. (2016). Ten years of eddy covariance measurements in Basel, Switzerland: Seasonal and interannual variabilities of urban co2 mole fraction and flux. *Journal of Geophysical Research: Atmospheres*, *121*(14), 8649–8667.
Shellito, P. J., Small, E. E., Colliander, A., Bindlish, R., Cosh, M. H., Berg, A. A., ... others (2016). SMAP soil moisture drying more rapid than observed in situ following rainfall events. *Geophysical research letters*, *43*(15), 8068–8075.
Somarakis, G., Stagakis, S., Chrysoulakis, Nektarios, Mesimäki, M., & Lehvävirta, S. (2019). Thinknature nature-based solutions handbook.
Stagakis, S., Chrysoulakis, N., Spyridakis, N., Feigenwinter, C., & Vogt, R. (2019). Eddy covariance measurements and source partitioning of co2 emissions in an urban environment: Application for heraklion, greece. *Atmospheric Environment*, *201*, 278–292.
Starke, P., Göbel, P., & Coldewey, W. (2010). Urban evaporation rates for water-permeable pavements. *Water Science and Technology*, *62*(5), 1161–1169.
Steeneveld, G.-J., van der Horst, S., & Heusinkveld, B. (2019). *Observing the surface radiation and energy balance, carbon dioxide and methane fluxes over the city centre of Amsterdam.* Presented at the EGU General Assembly 2020, Online, 4–8 May 2020. doi: https://doi-org.ezproxy.library.wur.nl/10.5194/egusphere-egu2020-1547
Stewart, I. D., & Oke, T. R. (2012). Local climate zones for urban temperature studies. *Bulletin of the American Meteorological Society*, *93*(12), 1879–1900.
Stone Jr, B., & Rodgers, M. O. (2001). Urban form and thermal efficiency: how the design of cities influences the urban heat island effect. *American Planning Association. Journal of the American Planning Association*, *67*(2), 186.
Taha, H. (1997). Urban climates and heat islands: albedo, evapotranspiration, and anthropogenic heat. *Energy and buildings*, *25*(2), 99–103.
Teuling, A. J., Seneviratne, S., Williams, C., & Troch, P. (2006). Observed timescales of evapotranspiration response to soil moisture. *Geophysical Research Letters*, *33*(23).
Theeuwes, N. E., Steeneveld, G.-J., Ronda, R. J., & Holtslag, A. A. (2017). A diagnostic equation for the daily maximum urban heat island effect for cities in northwestern Europe. *International Journal of Climatology*, *37*(1), 443–454.

Tingsanchali, T. (2012). Urban flood disaster management. *Procedia engineering*, *32*, 25–37.

Troch, P. A., Berne, A., Bogaart, P., Harman, C., Hilberts, A. G., Lyon, S. W., ... others (2013). The importance of hydraulic groundwater theory in catchment hydrology: The legacy of Wilfried Brutsaert and Jean-Yves Parlange. *Water Resources Research*, *49*(9), 5099–5116.

United Nations. (2018). *World urbanization prospects, the 2018 revision.* UN Department of Economic and Social Affairs.

Velasco, E., Perrusquia, R., Jiménez, E., Hernández, F., Camacho, P., Rodríguez, S., ... Molina, L. (2014). Sources and sinks of carbon dioxide in a neighborhood of Mexico City. *Atmospheric Environment*, *97*, 226–238.

Velasco, E., Pressley, S., Grivicke, R., Allwine, E., Molina, L. T., & Lamb, B. (2011). Energy balance in urban Mexico City: observation and parameterization during the MILAGRO/MCMA-2006 field campaign. *Theoretical and applied climatology*, *103*(3-4), 501–517.

Velasco, E., & Roth, M. (2010). Cities as net sources of co2: Review of atmospheric co2 exchange in urban environments measured by eddy covariance technique. *Geography Compass*, *4*(9), 1238–1259.

Velasco, E., Roth, M., Tan, S., Quak, M., Nabarro, S., & Norford, L. (2013). The role of vegetation in the co 2 flux from a tropical urban neighbourhood. *Atmospheric Chemistry and Physics*.

Vesala, T., Järvi, L., Launiainen, S., Sogachev, A., Rannik, Ü., Mammarella, I., ... others (2008). Surface–atmosphere interactions over complex urban terrain in Helsinki, Finland. *Tellus B: Chemical and Physical Meteorology*, *60*(2), 188–199.

Vulova, S., Meier, F., Rocha, A. D., Quanz, J., Nouri, H., & Kleinschmit, B. (2021). Modeling urban evapotranspiration using remote sensing, flux footprints, and artificial intelligence. *Science of The Total Environment*, 147293.

Wei, W., & Shu, J. (2020). Urban renewal can mitigate urban heat islands. *Geophysical Research Letters*.

Weng, Q., Lu, D., & Schubring, J. (2004). Estimation of land surface temperature–vegetation abundance relationship for urban heat island studies. *Remote sensing of Environment*, *89*(4), 467–483.

Wetzel, P. J., & Chang, J.-T. (1987). Concerning the relationship between evapotranspiration and soil moisture. *Journal of climate and applied meteorology*, *26*(1), 18–27.

Wilby, R. L. (2007). A review of climate change impacts on the built environment. *Built environment*, *33*(1), 31–45.

Williams, C. A., & Albertson, J. D. (2004). Soil moisture controls on canopy-scale water and carbon fluxes in an African savanna. *Water Resources Research*, *40*(9).

Wong, T. H. (2006). Water sensitive urban design-the journey thus far. *Australasian Journal of Water Resources*, *10*(3), 213–222.

Wouters, H., Demuzere, M., De Ridder, K., & van Lipzig, N. P. (2015). The impact of impervious water-storage parametrization on urban climate modelling. *Urban Climate*, *11*, 24–50.

Zhao, L., Lee, X., Smith, R. B., & Oleson, K. (2014). Strong contributions of local background climate to urban heat islands. *Nature*, *511*(7508), 216.

Zhou, Q. (2014). A review of sustainable urban drainage systems considering the climate change and urbanization impacts. *Water*, *6*(4), 976–992.

Zhou, Q., Leng, G., Su, J., & Ren, Y. (2019). Comparison of urbanization and climate change impacts on urban flood volumes: Importance of urban planning and drainage adaptation. *Science of the Total Environment*, *658*, 24–33.